

Understanding ZIF Particle Chemical Etching Dynamics and Morphology Manipulation: In-situ Liquid Phase Electron Microscopy and 3D Electron Tomography Application

Qiang Chang^{1,†}, *Dahai Yang*^{1,†}, *Xingyu Zhang*^{2,*}, *Zihao Ou*³, *Juyeong Kim*⁴, *Tong Liang*¹, *Junhao Chen*¹, *Sheng Cheng*¹, *Lixun Cheng*⁵, *Binghui Ge*⁵, *Edison Huixiang Ang*⁶, *Hongfa Xiang*¹, *Mufan Li*⁷, *Xiaohui Song*^{1,*}

¹School of Materials Science and Engineering, Hefei University of Technology, Anhui Province, 230009, China

²Department of Engineering & Mechanics, Beijing University of Technology, Beijing, 100124, China

³School of Materials Science and Engineering, Stanford University, Stanford, CA 94305, United States

⁴Department of Chemistry and Research Institute of Natural Sciences, Gyeongsang National University, Jinju 52828, South Korea

⁵Information Materials and Intelligent Sensing Laboratory of Anhui Province, Institutes of Physical Science and Information Technology, Anhui University, Hefei 230601, China

⁶Natural Sciences and Science Education, National Institute of Education, Nanyang Technological University, Singapore 637616, Singapore

⁷Institute of Physical Chemistry, the College of Chemistry and Molecular Engineering, Pecking University, Beijing, 100871, China

* To whom correspondence may be addressed: xingyu0711@bjut.edu.cn; xiaohuisong@hfut.edu.cn;

† These authors contribute equally to this work.

Content:

Supplementary notes 1-8

Supplementary discussion 1-2

Supporting Figures S1-29

Supporting tables 1-8

Supporting movies S1-9

Supplementary notes

Supplementary note 1: Zeolitic imidazolate framework-8 (ZIF-8) particle synthesis

Synthesis of ZIF-8 spindle with different concentrations of salt and imidazole (136.9 mM):

For example, the synthesis of ZIF-8 with a concentration of 136.9 mM zinc nitrate hexahydrate was adopted based on previous report¹, and described in detail in this section. In a typical experiment, the molar ratio of salt to 2-methylimidazole (2-MIM) was controlled at 1:10. First, weighed out 136.9 mM of $\text{Zn}(\text{NO}_3)_2 \cdot 6\text{H}_2\text{O}$ (0.4066 g) and 1.364 M of 2-MIM (1.12 g) and dispersed them in 10 mL of water, then dissolved them by sonication. Next, the zinc nitrate solution was mixed with the 2-MIM solution for 5 min. After letting it stand at room temperature for 5 h, the white liquid was transferred to a centrifuge tube with 2 mL of a methanol/ethanol (V=1:1) mixture added and centrifuged four times at a speed of 3000 rpm/min for 7 min each time. Lastly, the top liquid layer was discarded and the resulting sample was dried overnight in an oven at 55 °C (Supporting information Fig.S1-2).

Synthesis of ZIF-8 spindle with different concentrations of salt and imidazole (68.45 mM):

ZIF-8 was synthesized using a zinc nitrate hexahydrate concentration of 68.45 mM and a salt-to-2-methylimidazole molar ratio of 1:10. Firstly, 68.45 mM of $\text{Zn}(\text{NO}_3)_2 \cdot 6\text{H}_2\text{O}$ (0.2033 g) and 682 mM of 2-MIM (0.56 g) were dispersed separately in 10 mL of water and dissolved via sonication. Then, the zinc nitrate solution was added into 2-MIM and stirred for 5 min. After that, the mixture was left at room temperature for 5 h, and the resulting white liquid was transferred to a centrifuge tube. 2 mL of methanol/ethanol (V=1:1) mixture was added, and the mixture was centrifuged four times at a speed of 3000 rpm/min for 7 min each time. The supernatant was removed, and the resulting sample was dried overnight in an oven at 55 °C¹.

Synthesis of ZIF-8 dodecahedral structure with aqueous solvent system (Fig. S6 a-d): In this experiment, the molar ratio of salt to imidazole was controlled at 1:10. Firstly, 273.3 mM (0.3 g) $(\text{CH}_3\text{COO})_2\text{Zn} \cdot 2\text{H}_2\text{O}$ and 2.728 M (1.12 g) 2-MIM were dispersed in 5 mL of water and dissolved through sonication. Then, the zinc acetate solution was poured into 2-MIM and stirred for 20 s. After being allowed to stand at room temperature for 24 h, the white liquid was transferred to a centrifuge tube and 2 mL of methanol/ethanol (V=1:1) mixed solution was added. The sample was

centrifuged four times at a speed of 3000 rpm for 8 min each time. The supernatant was removed, and the obtained sample was dried in an oven overnight at 55°C¹.

Synthesis of ZIF-8 tetrahedral crystal structure with methanol/ethanol mixed solvent system

(Fig. S6 e-h): Firstly, 31.8 mM (0.189 g) $\text{Zn}(\text{NO}_3)_2 \cdot 6\text{H}_2\text{O}$ and 59.2 mM (0.426 g) PVP were dispersed in a 20 mL methanol/ethanol mixed solvent (V=1:1) via sonication. Then, 197.76 mM (0.328 g) 2-methylimidazole (1-MIM) and 197.76 mM (0.328 g) 2-MIM were dispersed in a 20 mL methanol/ethanol mixed solvent (V=1:1) by sonication. The imidazole solution was then added to the zinc nitrate solution, stirred for 20 s, and left to stand for 6 h. The supernatant was aspirated using a pipette, 30 mL ethanol was added and the mixture was dispersed by sonication, and then transferred to a centrifuge tube. The mixture was centrifuged at 2500 rpm/min for 8 min, the supernatant was aspirated using a pipette, 20 mL of ethanol was added, and the mixture was centrifuged at 2500 rpm/min for 8 min. This process was repeated twice at 1500 rpm/min for 8 min each time to remove the supernatant. The resulting sample was dried overnight in an oven at 55 °C.

Supplementary note 2: ZIF-8 etching experiments

Weak acid etching: ZIF-8 was etched using the method described in literature¹. In the etching experiment, regulating the pH of acidified xylenol orange tetrasodium salt (XO, AR) solution with hydrochloric acid titration (pH =3.61, 3.92), and the volume of XO solution was kept the same as the volume of ZIF-67 solution with pH = 3.61 for etching. First, 20 mg/mL (0.2 g) of XO was dissolved in 10 mL of water and 0.5 mL of hydrochloric acid was added. Then, 33 mg/mL (0.3482 g) of ZIF-8 was dissolved in 10.5 mL of water. The XO solution was added to the ZIF-8 solution and stirred for 30 min. Then, 10 mL of water was added to stop the reaction, followed by 5 mL of ethanol. The solution was transferred to a centrifuge tube and centrifuged at 5000 rpm/min for 10 min. The supernatant was removed using a pipette, and then 20 mL of water and 10 mL of ethanol were added. The solution was centrifuged at 4000 rpm/min for 10 min, and the supernatant was removed using a pipette. Finally, 30 mL of ethanol was added, and the solution was centrifuged at 3000 rpm/min for 10 min. The supernatant was removed, and the sample was dried in an oven overnight at 55 °C (Supporting information Fig.S8).

pH=3.92 etching of ZIF-8: First, 20 mg/mL (0.2 g) XO was dissolved in 10 mL of water and 0.3 mL of hydrochloric acid was added. Then, 20 mg/mL (0.0102 g) ZIF-8 was dissolved in 0.5 mL of water, and 0.5 mL of XO solution was added to the ZIF-8 solution and stirred for 30 min. Next, 2

mL of water and 2 mL of ethanol were added to stop the reaction, and the solution was transferred to a centrifuge tube and centrifuged at 4000 rpm/min for 10 min. The supernatant was removed using a pipette, and then 2 mL of water and 2 mL of ethanol were added and centrifuged at 3000 rpm/min for 10 min. The supernatant was removed using a pipette, and then 4 mL of ethanol was added and centrifuged at 3000 rpm/min for 10 min. The supernatant was removed, and the resulting sample was dried overnight at 55 °C in an oven.

Deionized water etching: 0.2 g of ZIF-8 was added in 30 mL of water and stand for 8 h followed by purifying the particles by adding 30 mL of water, then ultrasonic. Repeat this cleaning process for 10 times at a centrifugation rate of 7000-1000 rpm/min and lastly dried the samples in an oven at 55 °C overnight.

Supplementary note 3: ZIF-67 synthesis experiments

Synthesis of ZIF-67 dodecahedron crystal structure with different solution volumes (Fig. S6 e-h): For the synthesis of ZIF-67 with a total volume of 3 mL¹, the 243.69 mM (0.0607 g) of (CH₃COO)₂Co·4H₂O was first dissolved in 1 mL of water to form (CH₃COO)₂Co·4H₂O solution. Next 1.366 M (0.2243 g) of 2-MIM was added in 2 mL of water to obtain 2-MIM solution. Mixed the (CH₃COO)₂Co·4H₂O solution and 2-MIM solution together through stirring for 20 s, and let it stand undisturbed for 4 h. Afterwards, a transfer pipette was used to remove the supernatant and 10 mL of water was added for redispersion of particles by sonication. Then the solution was transferred into a centrifuge tube and centrifuged at 5000 rpm/min for 8 min. A transfer pipette was used to remove the supernatant, 2 mL of water and 5 mL of ethanol mixture was used to purify the particles at a centrifugation rate of 4000 rpm/min for 8 min. This step was repeated and centrifuged at 3000 rpm/min for 8 min. The supernatant was removed and the resulting sample was dried overnight in an oven at 55 °C (Supporting information Fig.S11).

Synthesis of ZIF-67 with a total volume of 15 mL¹: First dissolve 0.6 g (CH₃COO)₂Co·4H₂O in 5 mL of water to prepare a 481.76 mM solution. Then, prepare a 2.728 M (2.24g) 2-MIM solution in 10mL of water. Next, add the (CH₃COO)₂Co·4H₂O solution into the 2-MIM solution and stir for 20 seconds. Let the mixture sit for 5 hours, and then use a pipette to remove the supernatant. Add 10 mL of water, and disperse the solution using ultrasound. Transfer the solution to a centrifuge tube, and centrifuge at 5000 rpm/min for 8 min. Use a pipette to remove the supernatant, then add 2 mL of water and 5 mL of ethanol. Centrifuge again at 4000 rpm/min for 8 min, and repeat this step with

a centrifugation speed of 3000 rpm/min for 8 min. Remove the supernatant and dry the obtained sample overnight in a 55°C oven.

For the synthesis of ZIF-67 with a total volume of 60 mL:¹ 240.88 mM (1.2 g) of $(\text{CH}_3\text{COO})_2\text{Co}\cdot 4\text{H}_2\text{O}$ was dissolved in 20 mL of water for form $(\text{CH}_3\text{COO})_2\text{Co}\cdot 4\text{H}_2\text{O}$ solution, and 721.68 mM (2.37 g) of 2-MIM was dissolved in 40 mL of water to obtain the 2-MIM solution. Then the two solutions were mixed by stirring for 5 min, let to stand for 24 h. After that, the supernatant was removed using a pipette and the particles were purified by 10 mL of water and centrifuged at 5000 rpm/min for 8 min. Then 2 mL of water and 5 mL of ethanol were added and centrifuged at 4000 rpm/min for 8 min. Repeat this process at a centrifugation rate of 3000 rpm/min for 8 min to remove the supernatant then the resulting sample was dried in an oven overnight at 55 °C.

Synthesis of ZIF-67@ZIF-67: First 133.82 mM (1.0 g) of $(\text{CH}_3\text{COO})_2\text{Co}\cdot 4\text{H}_2\text{O}$ was dissolved in 30 mL of water, and 1.62 M (4.0 g) of 2-MIM solution was prepared in 30 mL of water. Then, the $(\text{CH}_3\text{COO})_2\text{Co}\cdot 4\text{H}_2\text{O}$ solution was added to the 2-MIM solution, stirred for 20 s, and left to stand for 5 h. The upper liquid was removed using a pipette, and 10 mL of water was added. The solution was centrifuged at 4000 rpm/min for 8 min, and the process was repeated at 3000 rpm/min for 8 min. The resulting solid sample was used as seed in the coating experiment. Next, the obtained seed was added to 15 mL of water and sonicated. Then, 267.65 mM (1.0 g) of $(\text{CH}_3\text{COO})_2\text{Co}\cdot 4\text{H}_2\text{O}$ was added to 15 mL of water, sonicated, and the ZIF-67 solution was added to the cobalt acetate solution. The mixture was stirred for 10 min, and 1.62 M (4.0 g) of 2-MIM was sonicated and dissolved in 30 mL of water. The cobalt acetate solution was then poured into the 2-MIM solution, stirred for 20 s, and left to stand for 5 h. The upper liquid was removed using a pipette, and 10 mL of water was added. The solution was then sonicated, transferred to a centrifuge tube, and centrifuged at 5000 rpm/min for 8 min. The upper liquid was removed using a pipette, and 2 mL of water and 5 mL of ethanol were added. The solution was centrifuged at 4000 rpm/min for 8 min, and the process was repeated at 3000 rpm/min for 8 min. The resulting solid sample was dried overnight in a 55 °C oven.

ZIF-67@PS (polystyrene spheres) synthesis:² 2 g of NaOH was dissolved in 18 g of water, and 70 mL of styrene was added to the solution. Then 1.25 g of PVP was added in the above mixture. Then 1 g of $\text{K}_2\text{S}_2\text{O}_8$ in 50 mL of water was dissolved and added into the mixture. The resultant solution was stirred for 30 min at 60 °C and filtered to obtain white PS beads. 0.2 g of PS bead was dissolved in 30 mL of water and 1 g of $\text{Co}(\text{CH}_3\text{COO})_2$ solution was added and mixed for 10 min.

Then, 4 g of 2-MIM dissolved in 30 mL of water was added to the PS-Co-styrene mixture and stirred for 5 min, then let it stand for 5 h before removing 40 mL of the upper liquid using a pipette and added 20 mL of water followed by centrifugation at 5000 rpm/min for 8min. Repeat the purification process using 20 mL of ethanol at a centrifugation rate of 4000 rpm/min, then 3000 rpm/min, and lastly at 2000 rpm/min. The resulting solid sample was dried overnight in an oven at 55 °C.

Supplementary note 4: ZIF-67 etching experiments

Weak acid etching: ZIF-67 was etched using the method described in the literature¹. In this experiment, regulating the pH of XO solution with hydrochloric acid titration (pH = 3.09, 3.25, 3.61), while keeping the total volume of the acidic XO etching solution the same as the volume of the ZIF-67 solution. The acidic XO solution was added to the ZIF-67 solution and stirred for 30 minutes. Then, 2 mL of water and 2 mL of ethanol were added to stop the reaction. The solution was transferred to a centrifuge tube and centrifuged at 4000 rpm/min for 10 minutes. The supernatant was removed using a pipette. Then, 2 mL of water and 2 mL of ethanol were added, and the mixture was centrifuged at 3000 rpm/min for 10 min. The supernatant was removed using a pipette. Finally, 4 mL of ethanol was added, and the mixture was centrifuged at 3000 rpm/min for 10 minutes. The supernatant was removed, and the resulting sample was dried overnight in a 55 °C oven (Supporting information Fig.S17).

ZIF-67@PS etching: 6 mg/mL (0.0304 g) of ZIF-67@PS was added in 5 mL of tetrahydrofuran and sonicated for 5 min, let it stand for 2 h followed by centrifugation at a rate of 500 rpm/min for 10 min. The resulting solid sample was dried in an oven overnight at 55 °C.

Supplementary note 5: Basic characterizations of materials

The surface morphology of the sample was observed using a Field Emission Scanning Electron Microscope (FE-SEM), ZEISS Gemini 500 model, with a secondary electron resolution of ≤ 0.5 nm (15 kV) and ≤ 0.9 nm (1 kV), and a magnification range of 50-200,000. The acceleration voltage range was 0.02-30 kV, and the element analysis range was Be-Cf. For SEM sample preparation, a small amount of dried sample was taken in a 5 mL test tube, and 2 mL of ethanol was added and sonicated to disperse the sample. 30 μ L of the solution was then pipetted onto a silicon wafer and allowed to air dry naturally.

Transmission Electron Microscopy (TEM) was used to observe the microstructure of the sample. The instrument used was a JEM-2100F at 200 kV, and magnification ranging from 300 to 150000.

The CCD camera had a resolution of at least 11 million pixels, and beam drift was less than 1nm/min. TEM sample preparation involved taking a small amount of dried sample in a 5 mL test tube, adding 2 mL of ethanol, sonicating to disperse the sample, and then using a pipette to drop 30 μL of the solution onto a TEM copper grid, followed by air-drying.

The *in-situ* liquid-phase TEM imaging experiments were conducted in a 120 kV JEM-1400flash TEM (JEOL Ltd., Tokyo, Japan) equipped with a Gatan camera. The *in-situ* image series were acquired at a rate of 5 frames per second with a dose rate range of 7.0-8.4 $\text{e}^- \text{\AA}^{-2} \text{s}^{-1}$.

X-ray diffraction (XRD) was used to perform phase analysis on the samples using a SmartLab instrument with an incident slit ranging from 0.05 to 7 mm that is automatically adjustable with a 0.01 mm step. The XRD testing conditions for all samples in this experiment were as follows: copper target, scan angle of 2-7 $^\circ$, and a scan rate of 6 $^\circ/\text{min}$.

Supplementary note 6: nanoparticle size survey

Regarding the particle size analysis involved in this paper, we measured the nanoparticles in multiple TEM and SEM images and analyzed their size distribution based on the measurement results (shown in the table below) to obtain the particle size distribution curve. We hope to obtain a quantitative relationship between the trend of particle size distribution and the synthesis condition parameters.

Supplementary note 7: Three-dimensional (3D) tomography experiments

A series of tilt images of a MOF particle were acquired using a JEM-1400flash. A low electron beam dose rate (7.0-8.4 $\text{e}^- \text{\AA}^{-2} \text{s}^{-1}$) was applied using spot size 3. Each image was collected with a 3 s exposure time. The tilt angle ranged from -42 $^\circ$ to 64 $^\circ$ (ZIF-8 spindle) and -52 $^\circ$ to 56 $^\circ$ (ZIF-8 star) and -62 $^\circ$ to 46 $^\circ$ (ZIF-67 core-shell) in 2 $^\circ$ increments. Segmentation and 3D tomography analysis were performed in ImageJ/FIJI³ and Amira 6.4 (FEI) .

Supplementary note 8: volume calculation and etching speed calculation

Regarding volume calculation: We used 3D Max software to model the structures, ensuring that the dimensions of the model matched the results obtained from TEM and SEM measurements. Then, the actual volume of the spindle-shaped and star-shaped structures we used in the experiment before etching could be obtained by calculating the volume of the model. The volume calculation was performed to quantitatively determine the etching rate. According to 3D tomography and ex situ

etching experiments control (pH = 3.61 for all etching), the volume after etching (V_e) for different morphologies are:

ZIF-8 hollow spindle $V_{e1} = 0.177 \times 10^6 \text{ nm}^3$ (according to 3D tomography)

etching time $t_1 = 60 \text{ s}$ (according to ex situ etching experiment)

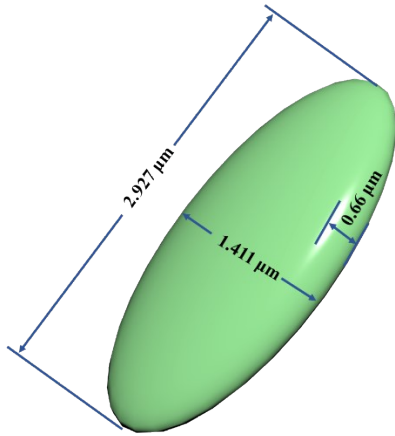
ZIF-8 hollow star $V_{e2} = 0.237 \times 10^6 \text{ nm}^3$ (according to 3D tomography)

etching time $t_2 = 120 \text{ s}$ (according to ex-situ etching experiment)

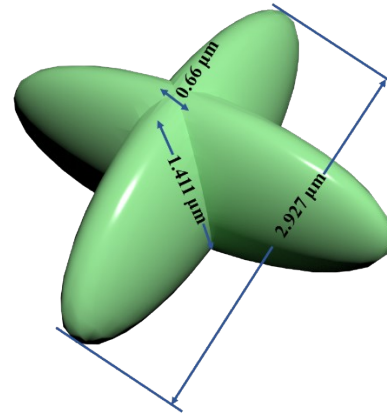
ZIF-67 hollow core-shell $V_{e3} = 0.213 \times 10^6 \text{ nm}^3$ (according to 3D tomography)

$V_{o3} = 8.52 \times 10^6 \text{ nm}^3$ (according to 3D tomography)

etching time $t_3 = 240 \text{ seconds}$ (according to ex situ etching experiment)



Volume of ZIF-8 spindle: $V_{o1} = 1400448 \text{ nm}^3$



Volume of ZIF-8 star: $V_{o2} = 2410972 \text{ nm}^3$

Etching Speed (\bar{v}) = $(V_o - V_e)/t$

Etching Speed of ZIF-8 spindle: $\bar{v}_1 = 2.03 \times 10^4 \text{ nm}^3/\text{s}$ (pH = 3.61)

Etching Speed of ZIF-8 star: $\bar{v}_2 = 1.81 \times 10^4 \text{ nm}^3/\text{s}$ (pH = 3.61)

Etching Speed of ZIF-67: $\bar{v}_3 = 3.46 \times 10^4 \text{ nm}^3/\text{s}$ (pH = 3.61)

Supplementary discussion 1 :

Typically, cobalt acetate was used as the cobalt source and 2-MIM was used as the organic ligand in the synthesis experiment in aqueous solution (Fig. S15 a-b). In the experiment, the total volume of the solution was controlled to vary from 3 mL (Supplementary Table 3) to 15 mL (Supplementary Table 4) and 60 mL (Supplementary Table 5), while keeping the molar concentration of each substance and other parameters constant (Fig. S11). The experimental results showed that the morphology and size of the obtained ZIF-67 polyhedron particles were correlated with the total volume of the solution (Fig. S15 c-j). i) As the total volume of the solution increased, the particle size distribution gradually became larger, indicating that the size range of ZIF-67 became larger; ii) As the total volume of the solution increased, the morphology differences of ZIF-67 became greater, and the defects of polyhedron became more apparent (Fig. S12-14). The above results indicate that the nucleation and growth processes of ZIF-67 were greatly affected by the total volume of the solution, manifested as local concentration differences, density gradients of particle growth environment, and the complexity of the overall liquid phase growth environment. This suggests that controlling the total volume of the solution is necessary and an important means to control the synthesis of monodispersed ZIF-67 particles.

In addition to the synthesis of ZIF particles themselves, using ZIFs to encapsulate other materials or NPs as a means of designing composite materials is also a popular research direction . Therefore, this study also investigated the effects of different shapes, sizes, and materials of NPs on the morphology of the resulting core-shell particles when they were encapsulated by ZIF-67, as well as their effects on the morphology of ZIF-67. We chose different NPs as the objects to be encapsulated, including ZIF-67 NPs, polystyrene spheres (PS) while ensuring that all other experimental conditions were the same (Fig. S15 j-m). The experimental results in Fig. S15 j-k show that ZIF-67@ZIF-67 has the smallest particle size distribution and the most complete structure, while the particle size distributions of ZIF-67@PS are relatively large.

Supplementary discussion 2 : (Regarding to beam damage to MOF particles in tomography)

Through our literature review³⁻⁵, we found that ZIF particles generally exhibit instability during HRTEM or HRSTEM characterization due to susceptibility to electron beam damage (normally, it's stable when the dose rate is from $1 \text{ e}^{-}\text{\AA}^{-2}\text{s}^{-1}$ to $3.5 \text{ e}^{-}\text{\AA}^{-2}\text{s}^{-1}$). This is attributed to the intense electron beam at high-resolution conditions, which can affect the material's stability at the atomic scale. However, in our experiments, the particles are already at the micrometer scale, and our focus is on morphological changes in micro scale. Thus, we did not perform atomic-scale imaging. We believe this is the reason we did not observe any changes in the morphology of ZIF particles in our experiments. As it is reported⁶, the MOF particles show beam damage at 200 kV above a cumulative electron dose (or total fluence) of $400 \text{ e}^{-}\text{\AA}^{-2}$. However, it is the case for in situ liquid phase TEM imaging which is complicated. For normal imaging in low magnification around $10 \text{ e}^{-}\text{\AA}^{-2}$ is available based on our previous experiments⁷ as well as other literatures^{8, 9}.

Supporting Figures S1-S25

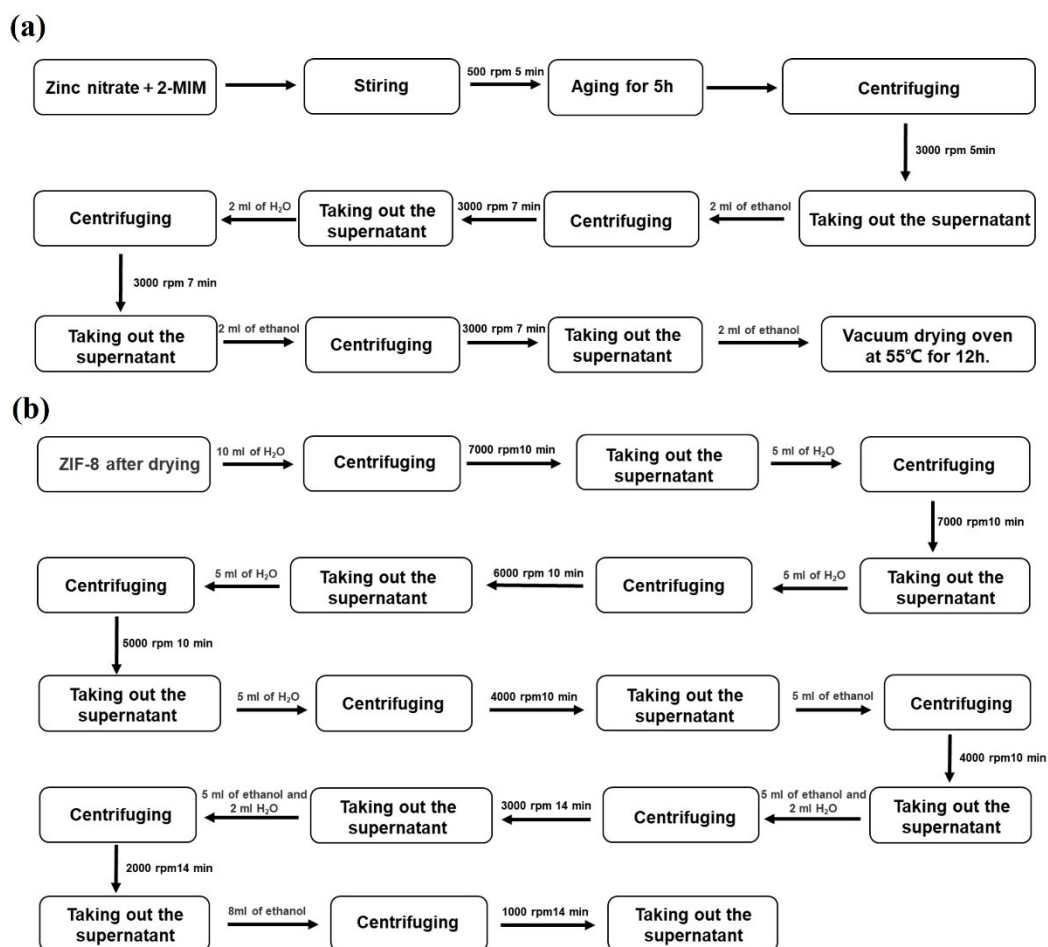


Fig. S1 Flow chart of synthesis experiment (a) and separation and purification of ZIF-8 (b).

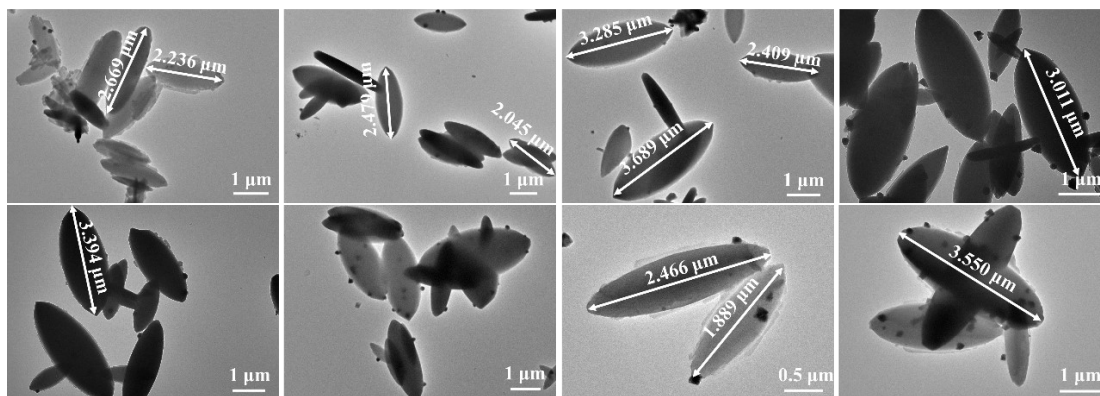


Fig. S2 TEM images of the ZIF-8 spindle.

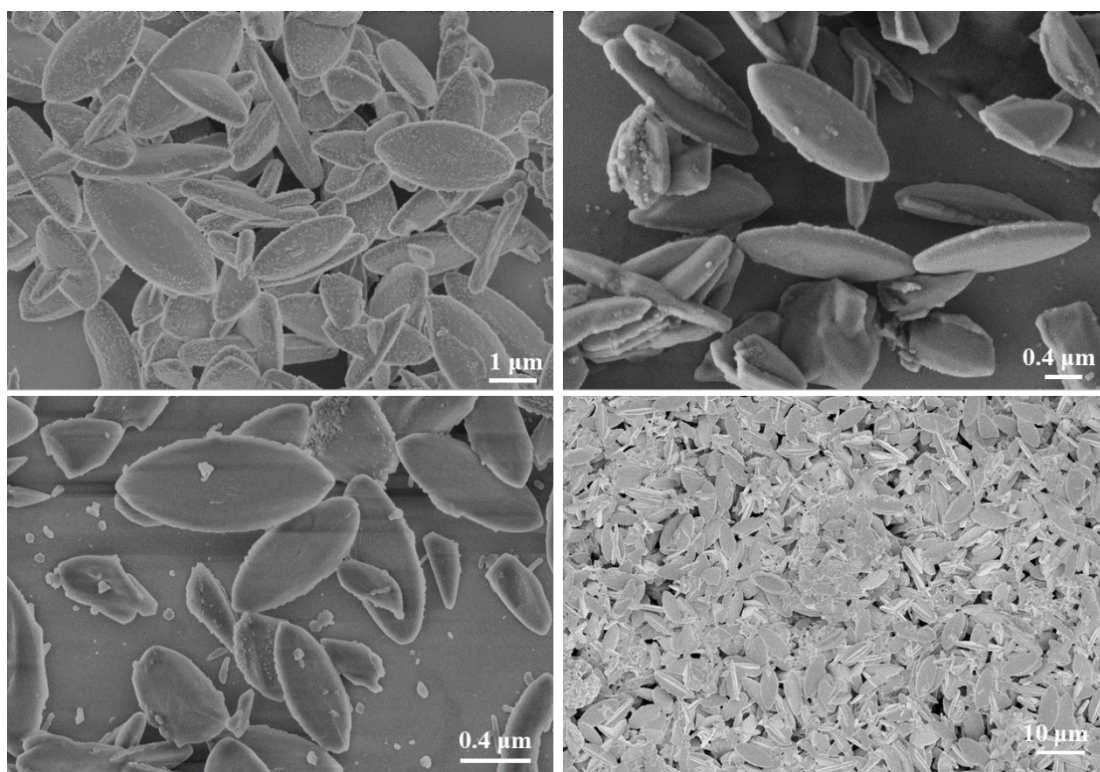


Fig. S3 SEM images of the ZIF-8 spindle

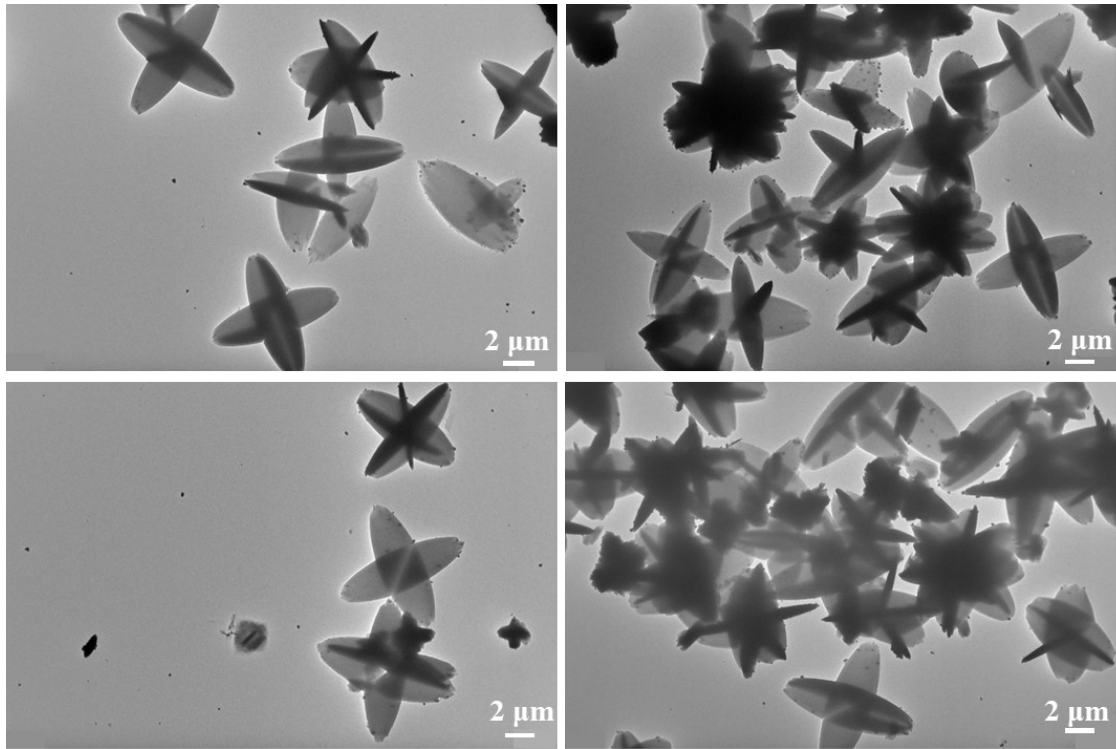


Fig. S4 TEM images of the ZIF-8 star

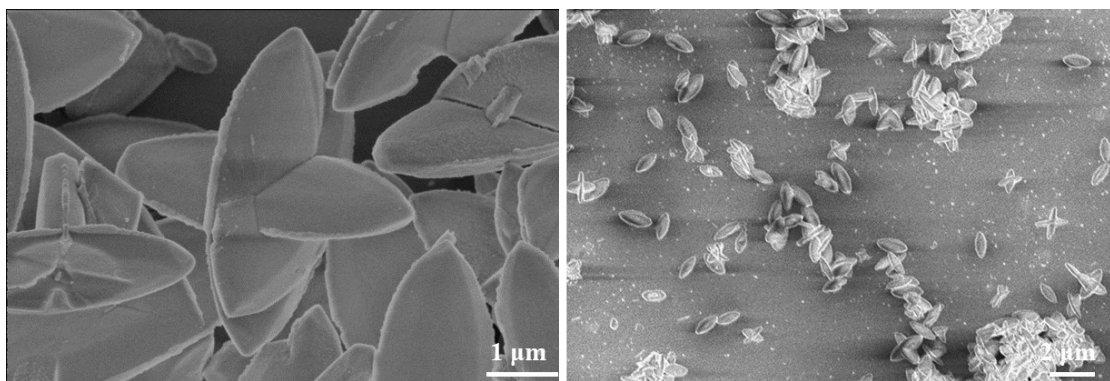


Fig. S5 SEM images of the ZIF-8 star

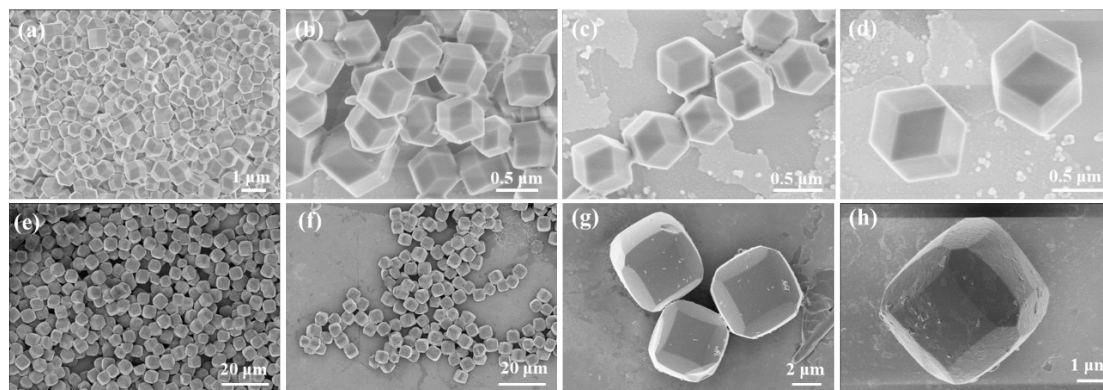


Fig. S6 SEM images of ZIF-8 polyhedron. (a-d) Aqueous synthesis of ZIF-8. (e-h) Alcohol phase synthesis of ZIF-8

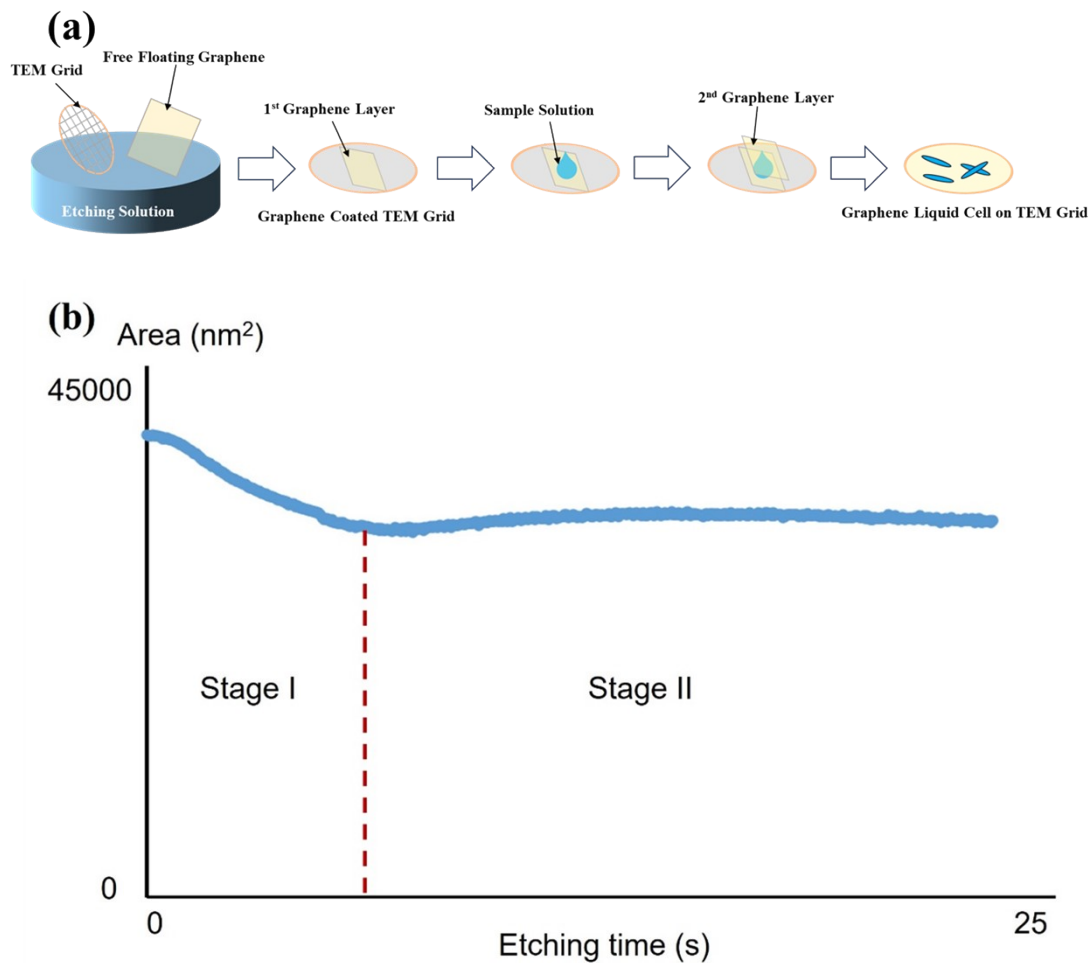


Fig. S7 (a) The in-situ TEM etch experiment graphene liquid cell design: flow chart of in-situ TEM sample preparation^{10, 11}. (b) histogram of ZIF-8 spindles particle surface area change with etching time. According to the image it is clear to see that the etching process was a two-step process. Note: the method of we followed was developed by Prof. Paul Alivisato's research group. The details are shown in the cited paper.¹²

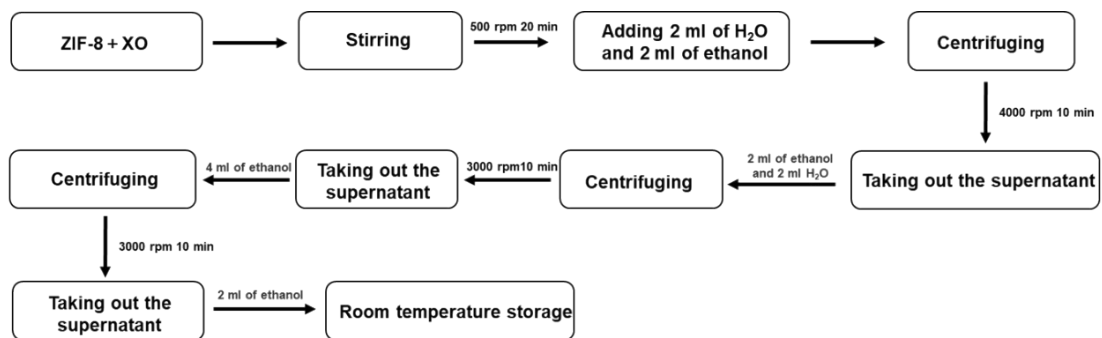


Fig. S8 Flow chart of ZIF-8 spindle etching experiment

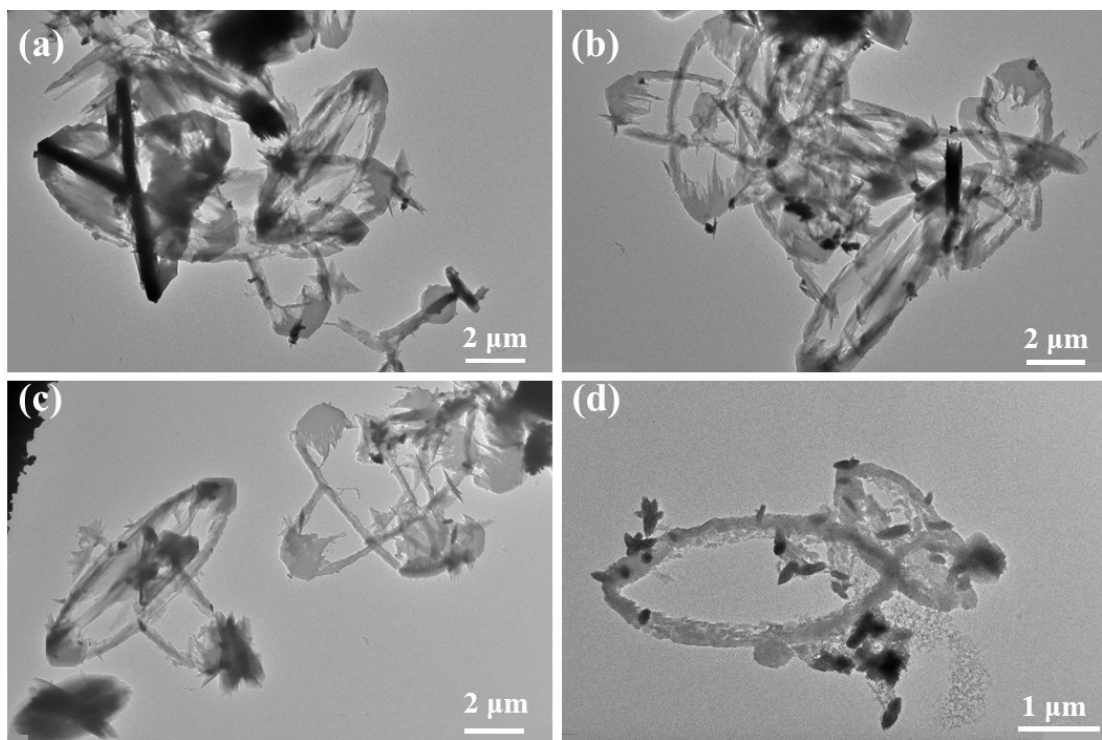


Fig. S9 TEM images of etched ZIF-8 spindle.

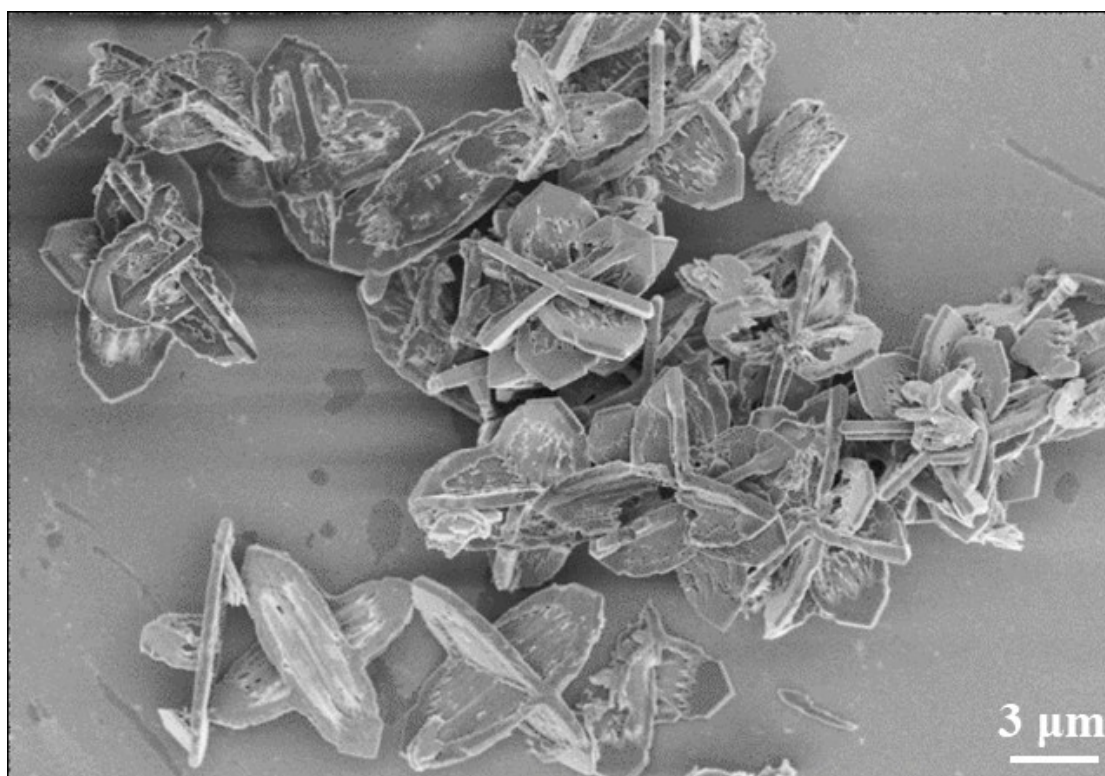


Fig. S10 SEM image of etched ZIF-8 spindle.

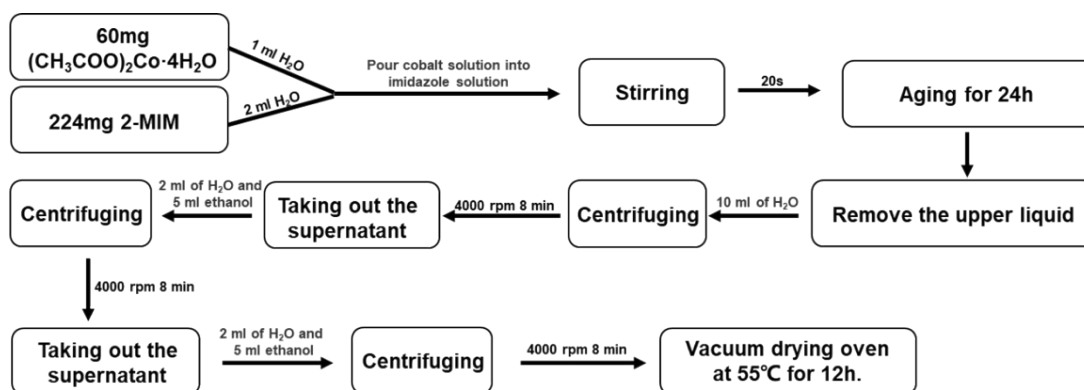


Fig. S11 Flow chart of ZIF-67 synthesis experiment.

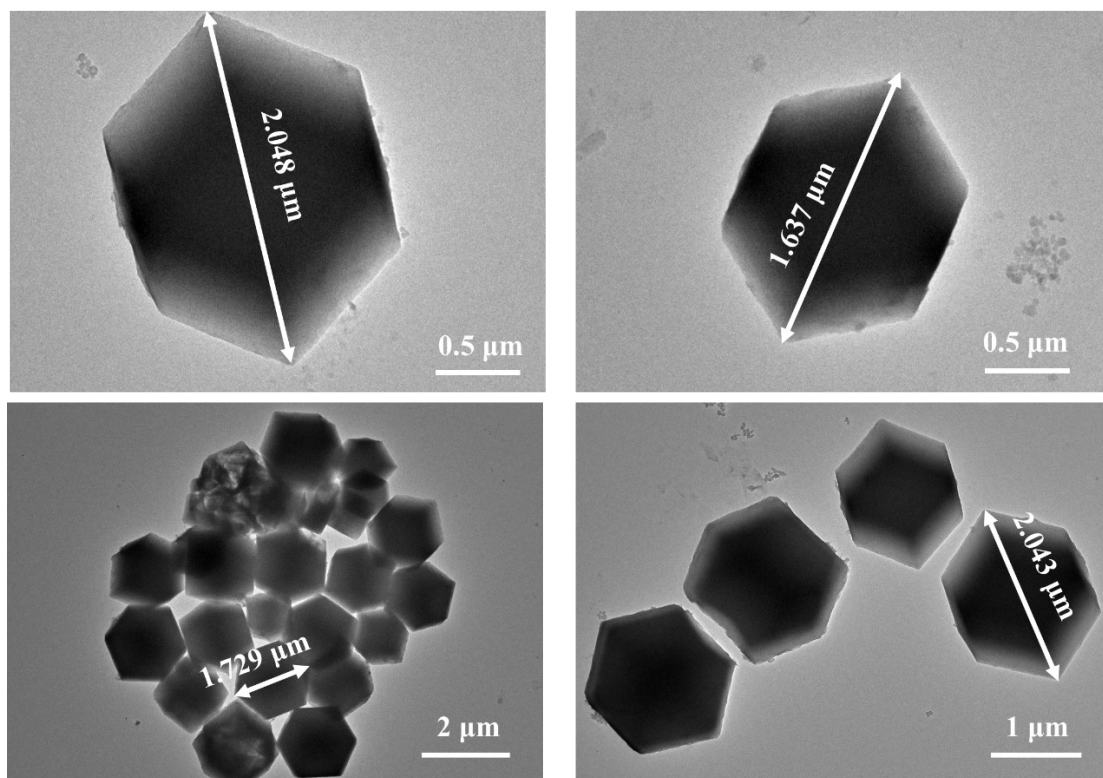


Fig. S12 TEM images of ZIF-67 synthesized in aqueous solution (total synthesis volume 3mL)

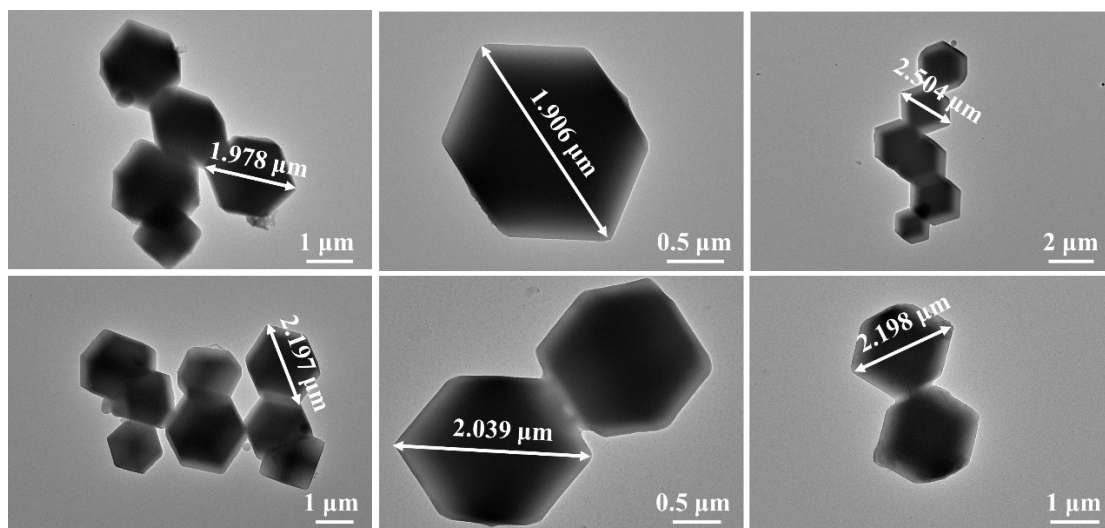


Fig. S13 TEM images of ZIF-67 synthesized in aqueous solution (total synthesis volume 15mL)

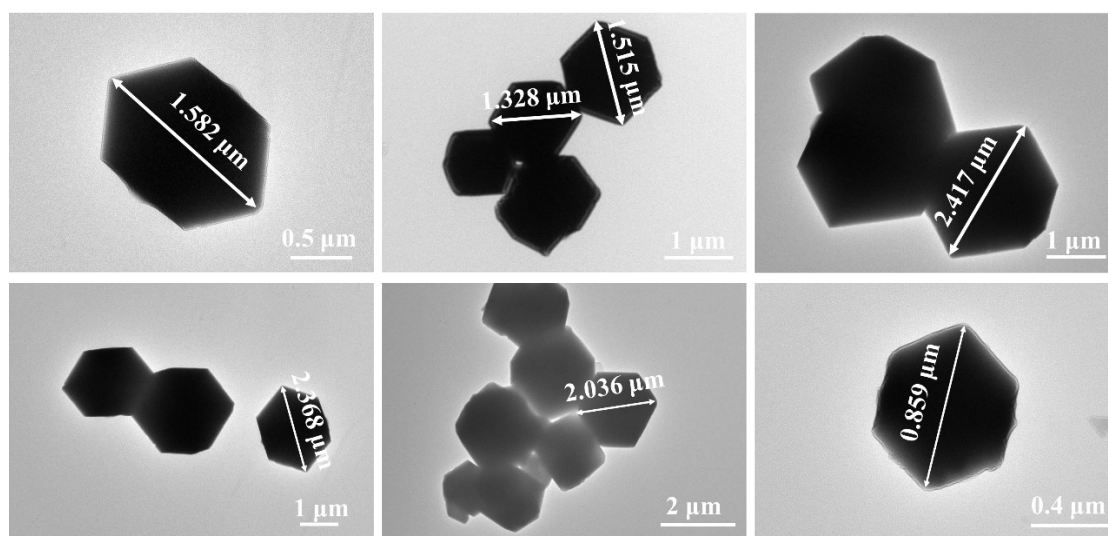


Fig. S14 TEM images of ZIF-67 synthesized in aqueous solution (total synthesis volume 60 mL).

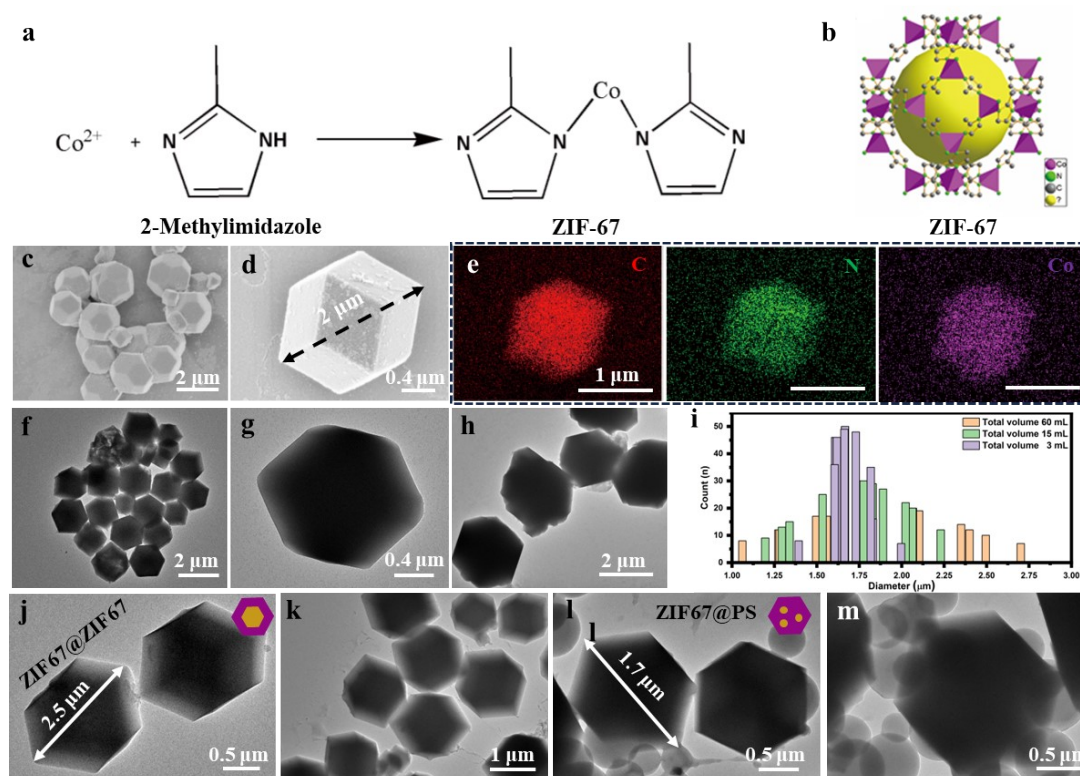


Fig. S15 ZIF-67 particles with different morphologies synthesized under different conditions. **a**. Synthesis reaction equation. **b**. ZIF-67 molecular structural formula. **c-d**. SEM images polyhedron shaped ZIF-67 particles. **e**. EDX maps of ZIF-67 particle. **f-h**. TEM images polyhedron shaped ZIF-67 particles. **i**. The survey of ZIF-67 particles size distribution based on the total volume difference in synthesis. **j-m**. TEM images of core-shell NPs using ZIF-67 to coat ZIF-67, polystyrene particles respectively.

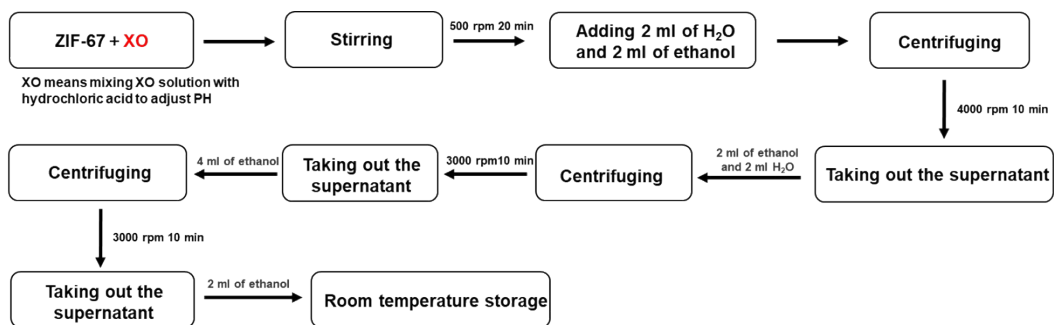


Fig. S16 ZIF-67 etching experiment flow chart.

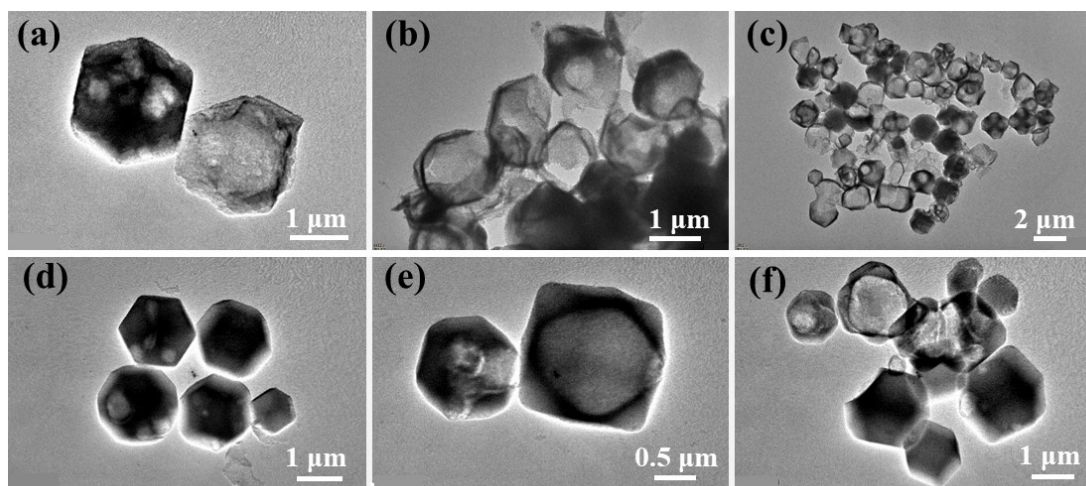


Fig. S17 TEM images of ZIF 67 etching under different pH conditions: pH=3.09 (a-c) and pH=3.61 (d-f).

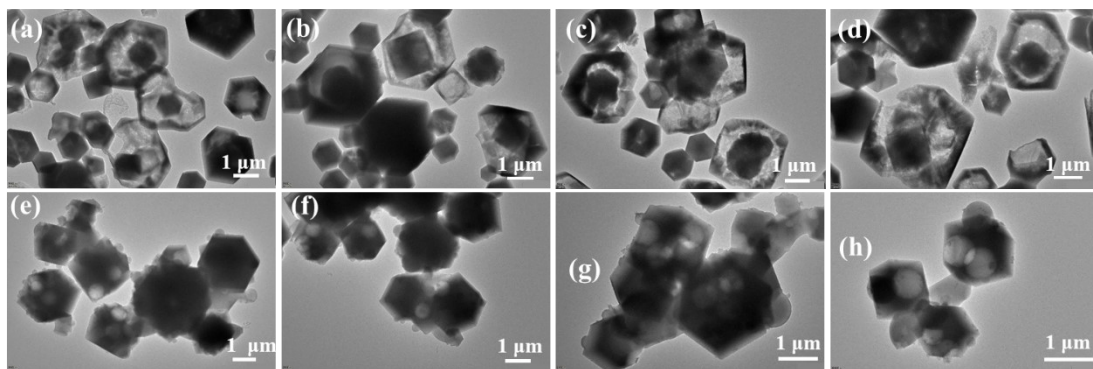


Fig. S18 ZIF-67 TEM images of etching different coated materials. (a-d) ZIF-67@ZIF-67 after etching and (e-h) ZIF-67@PS after etching.

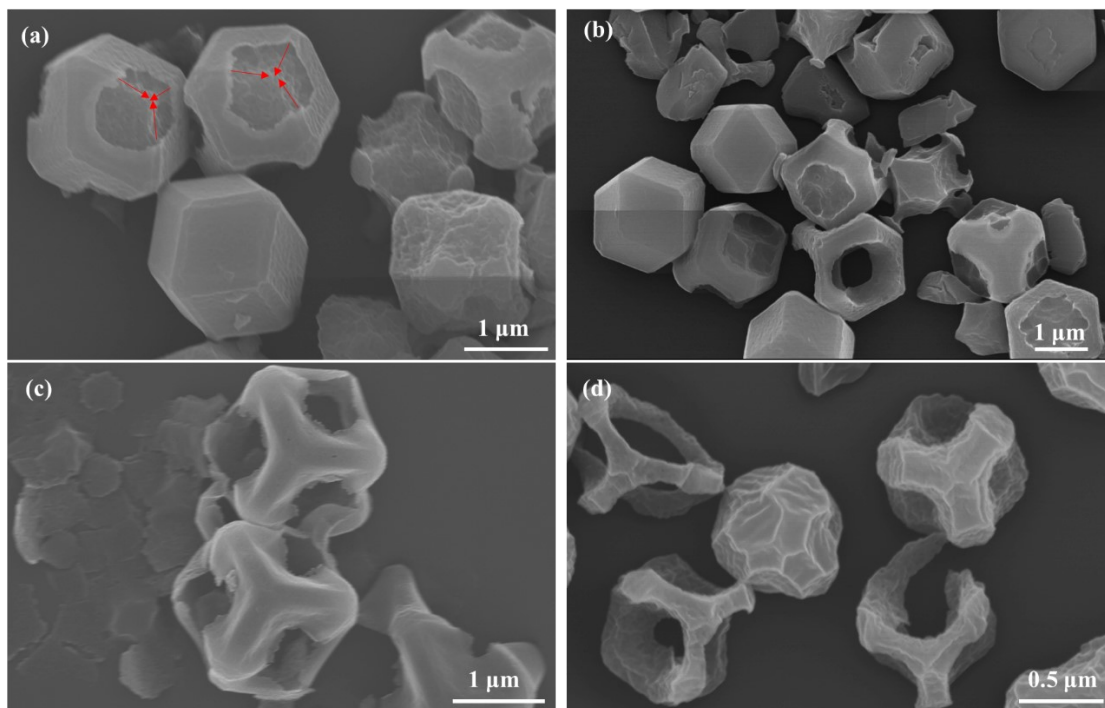


Fig. S19 SEM images of ZIF-67 in pH=2.39 solution after etching time of 5 min (a-b) and 10 min (c-d).

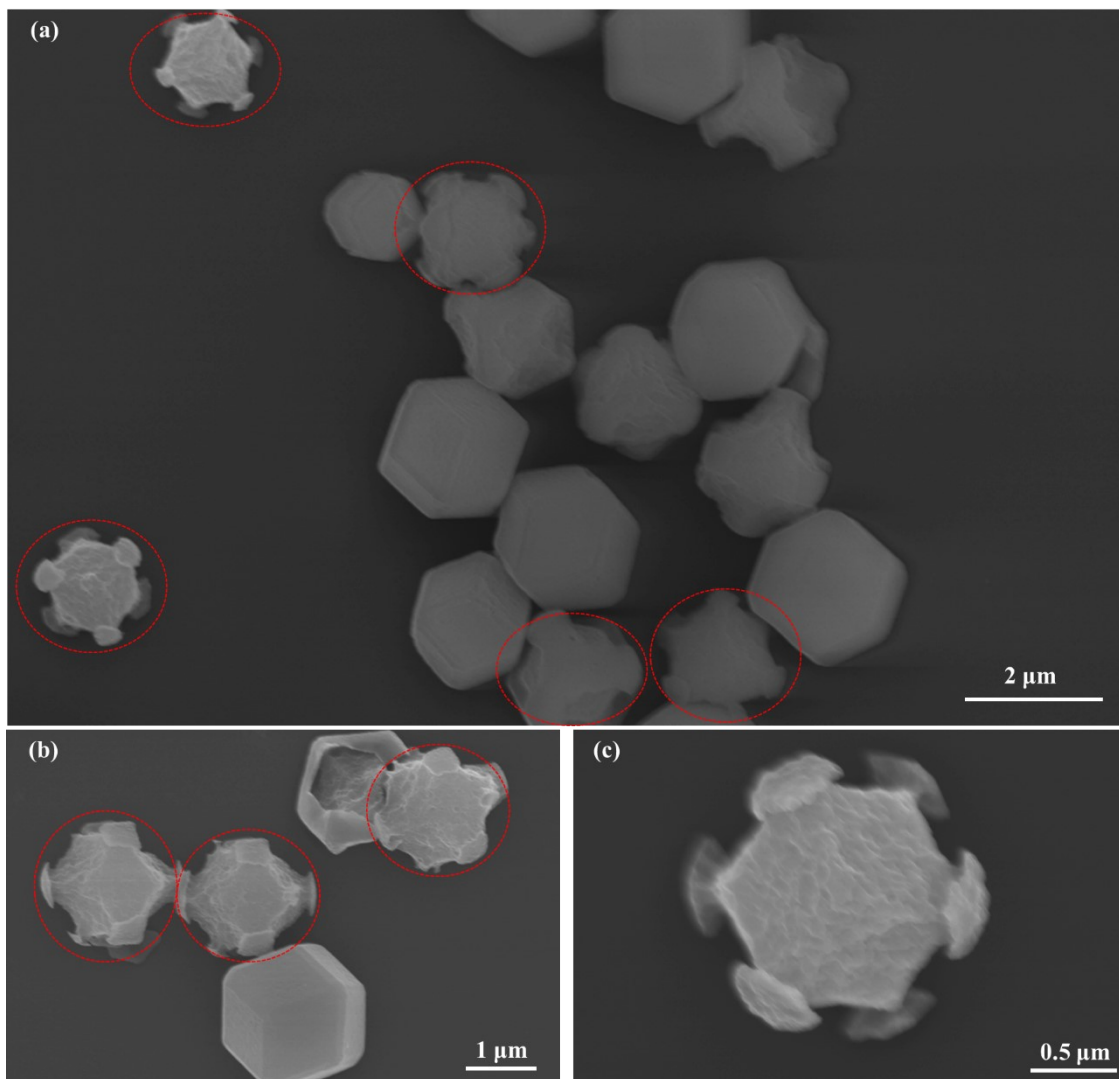


Fig. S20 SEM images of the final morphology of the ZIF-67 after 30 min etching in pH=2.39 solution.

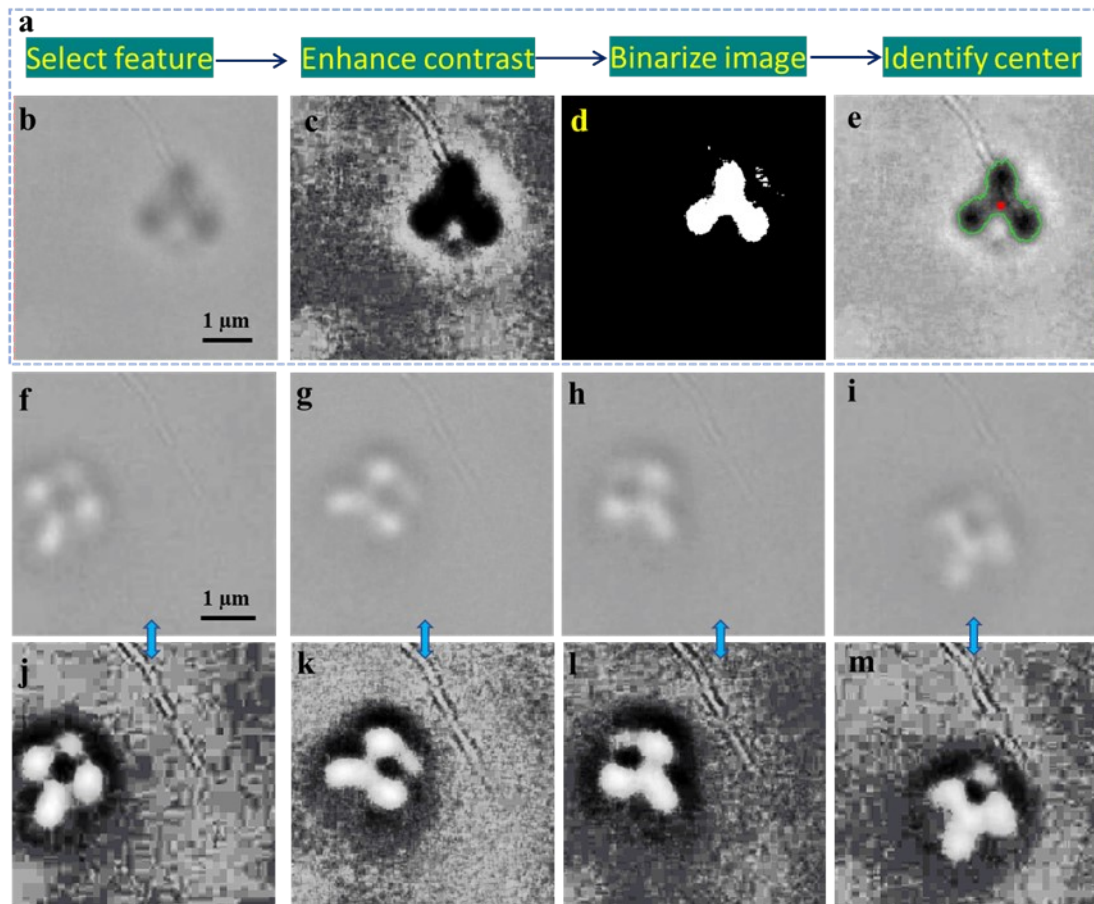


Fig S21. (a) flow chart showing the procedure of particle tracking process by using MATLAB coding method; (b-e) the corresponding images as shown in the flow chart; (f-i) the snapshots of ZIF microbox particles from the in-situ TEM movies S5; and (j-m) the corresponding images after tracking. This is the demonstration showing how we get the particle's movement dynamics.

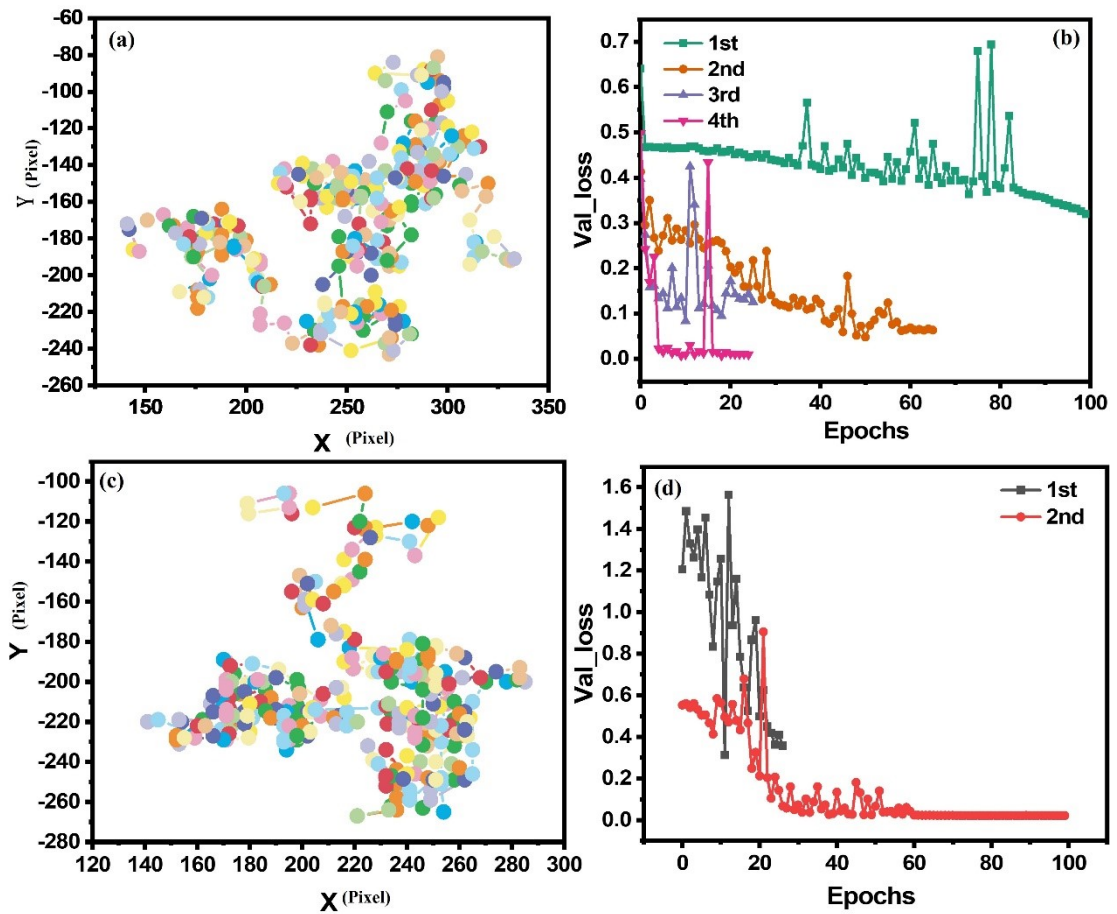


Fig S22. (a) the trajectory of ZIF67 microbox particle in motion of translation; (b) the loss function of data training in deep learning; (c) the trajectory of ZIF67 polyhedral particle in motion of translation; (d) the loss function of data training in deep learning. It is clear to see that microbox particle motion displacement is smaller than that of polyhedral particle.

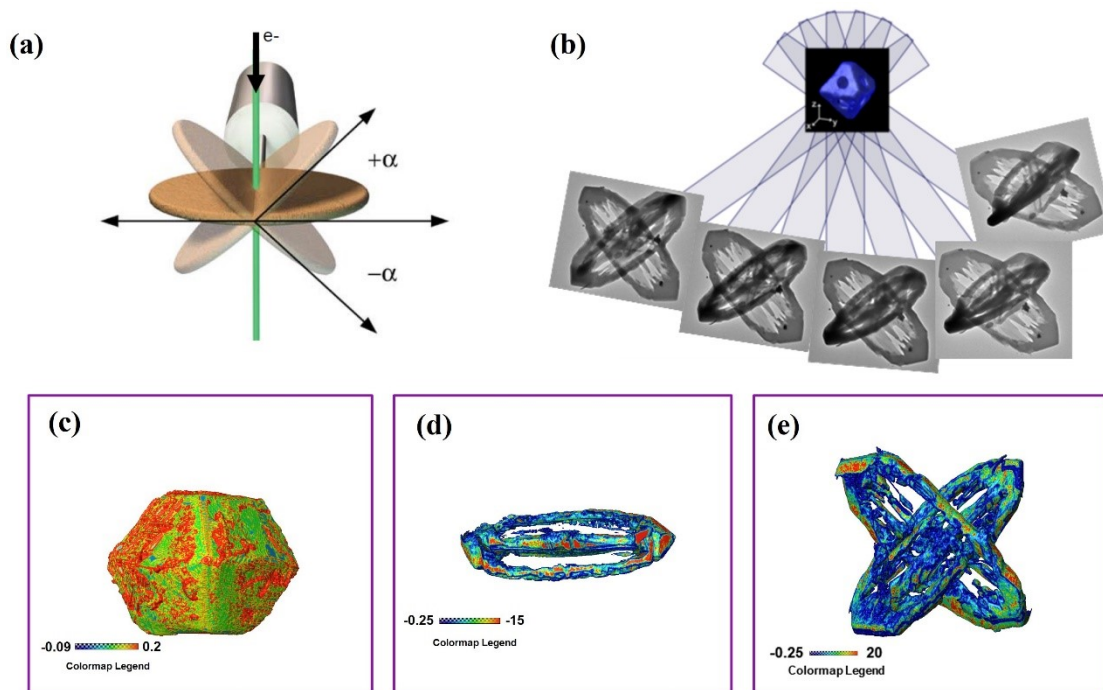


Fig. S23 (a-b) 3D tomography experiment of the ZIF reconstruction, and 3D curvature color map of different hollow particles: (c) ZIF-67@ZIF-67, (d) ZIF-8 spindle, (e) ZIF-8 star after etching.

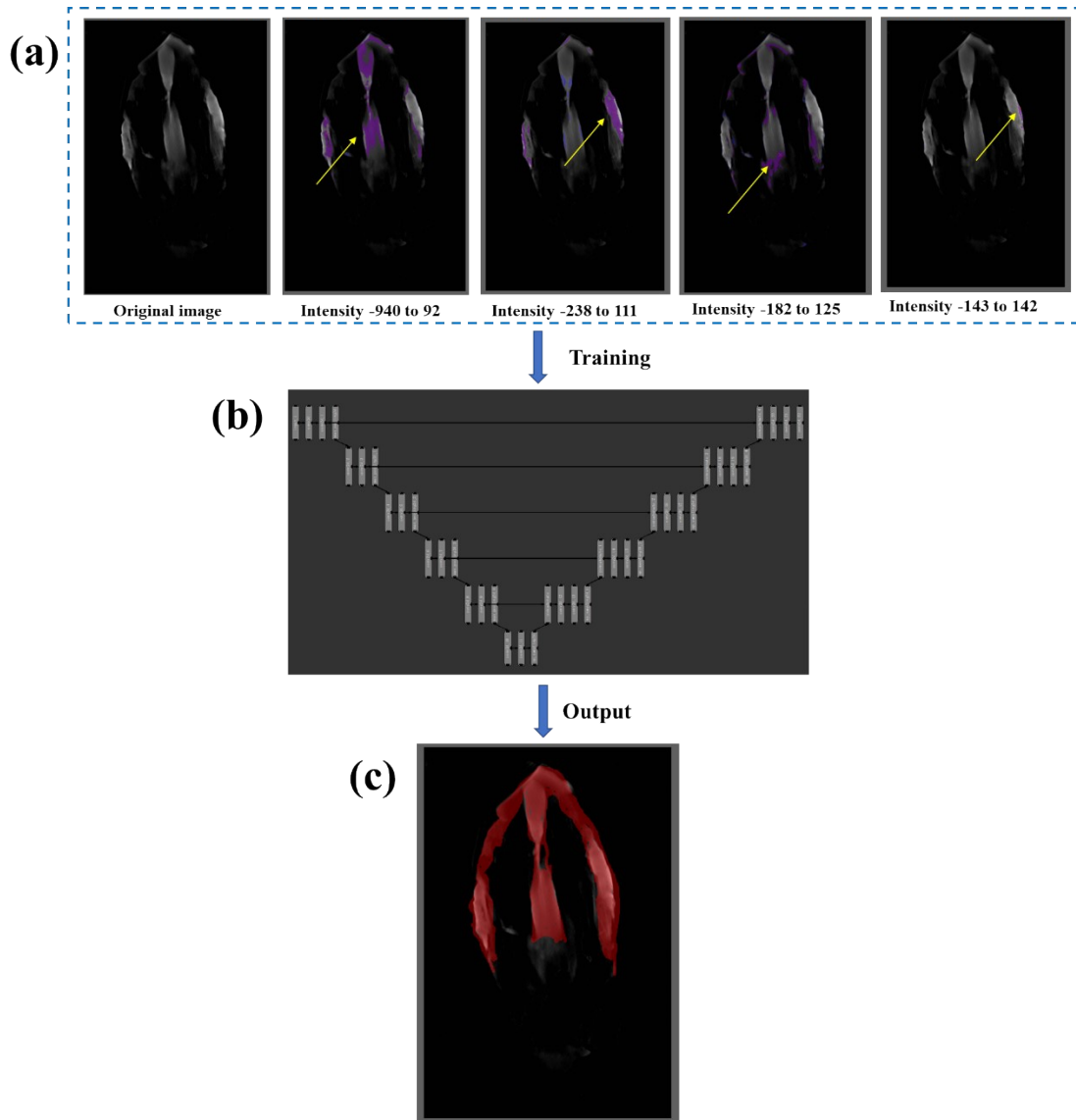


Fig. 24 (a-c) Working flow of 3D segmentation by using deep learning method which is applied to one slice in yz plane (slice No. 213). Figure *a* shows the thresholding process based on local resolution intensity value, which needs to be done many times to correct the tracking result; Figure *b* shows the deep learning mode (from Dragonfly software) by using the result of *a* as a training process, which will give the accurate segmentate as shown in figure *c*. ZIF-8 spindle particle.

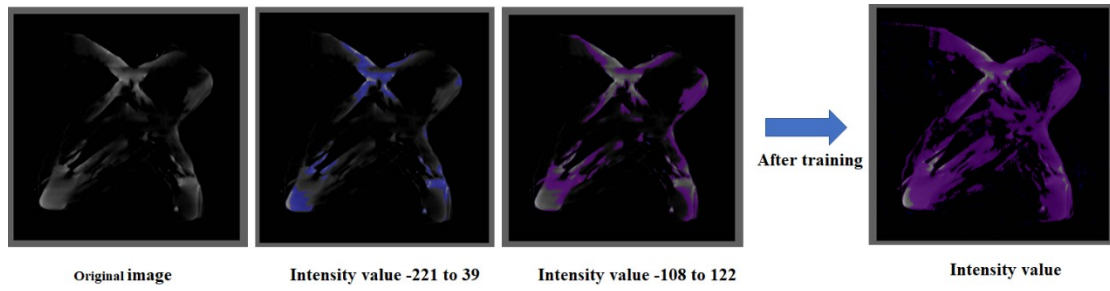


Fig. 25 Working flow of 3D segmentation by using deep learning method which is applied to one slice in yz plane (slice No. 262). ZIF-8 star particle.

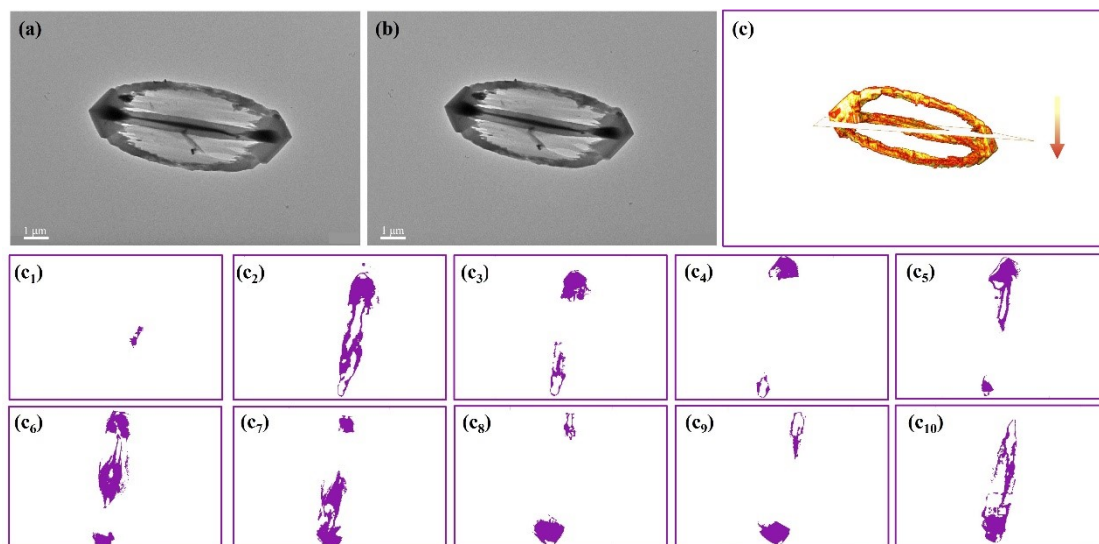
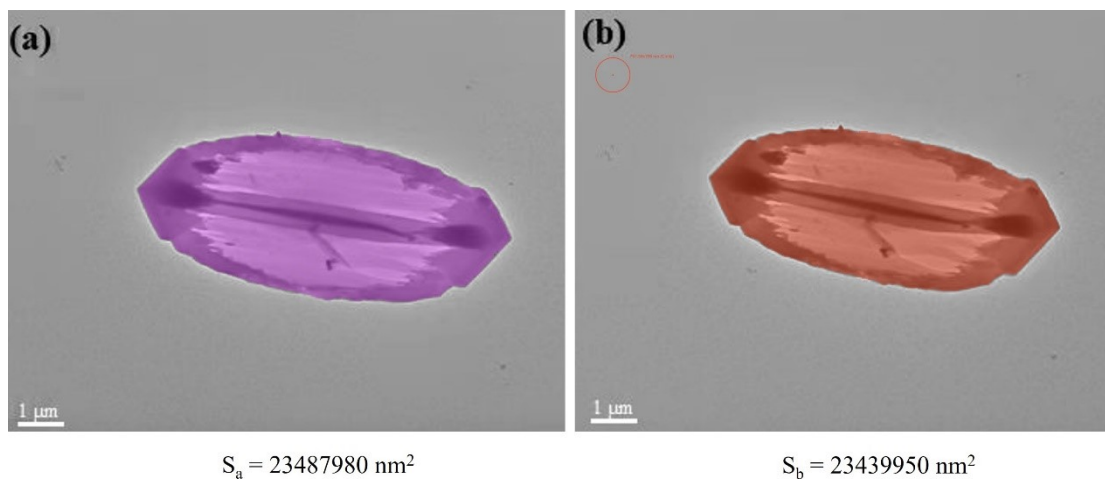


Fig. S26 (a) ZIF-8 hollow spindle Before tilting and (b) after tilting. (c) slicing in Z axis direction, (c₁-c₁₀) images of different slices while slice number is 73, 98, 123, 148, 173, 198, 223, 248, 273, 298. According to the slices it is clear to see that the inner domain of ZIF-8 spindle is a kind of core-shell morphology due to the hollow behavior.



$$S_a/S_b = 1.00204$$
$$\lambda \text{ (shrinking rate)} = (1.00204 - 1) \times 100\% = 0.204\%$$

Fig. S27 (a) TEM images of ZIF-8 hollow spindle before tilting and (b) after tilting in electron tomography experiments. The particle has been traced to calculate area change. The shrinking rate (λ) is 0.204%, which is calculated by using Dragonfly software.

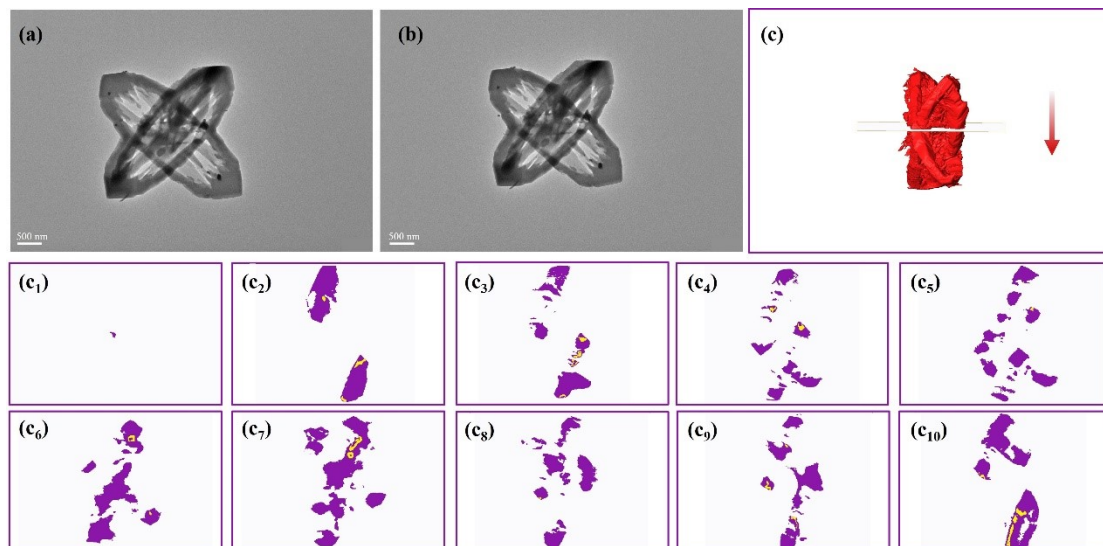


Fig. S28 (a) ZIF-8 hollow star Before tilting and (b) after tilting. (c) slicing in Z axis direction, and (c₁-c₁₀) images of different slices while slice number is 40, 75, 110, 145, 180, 215, 250, 285, 320, 355. According to the slices it is clear to see that the inner domain of ZIF-8 star is a kind of core-shell morphology due to the hollow behavior.

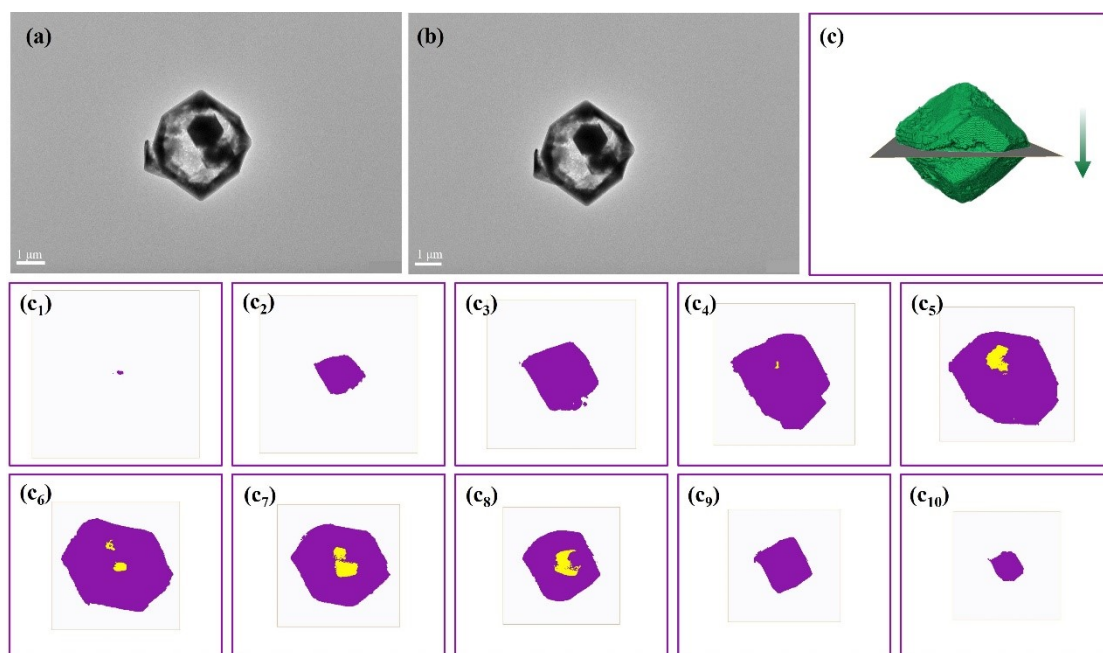


Fig. S29 (a) ZIF-67 hollow core-shell Before tilting and (b) after tilting. (c) slicing in Z axis direction, (c1-c10) images of different slices while slice number is 33, 61, 89, 117, 145, 173, 201, 229, 257, 285. According to the slices it is clear to see that the ZIF-67 inner domain is a kind of core-shell morphology due to the hollow behavior.

Supplementary Tables

Table 1. Size survey of ZIF-8 spindle particles

Count (n)	Diameter (D μm)
24	3.662
22	3.697
8	2.948
3	4.014
30	3.429
25	3.273
30	3.473
29	3.503
15	3.092
22	3.211
21	3.728

Tips: **n** indicates the number of statistical particles; **D** is the diameter of the particle.

Table 2. Size survey of ZIF-8 star particles

Count (n)	Diameter (D μm)
29	3.408
28	3.675
17	2.971
21	3.067
15	2.906
4	4.502
27	3.547
16	2.949
25	3.829
25	3.824
20	3.952

Tips: **n** indicates the number of statistical particles; **D** is the diameter of the particle.

Table 3. Size survey of ZIF-67 particles (Total synthesis volume 3mL)

Count (n)	Diameter (D μm)
16	1.787
35	1.774
46	1.564
7	1.953
48	1.686
46	1.579
8	1.349
50	1.622
46	1.574
49	1.619
36	1.561

Tips: **n** indicates the number of statistical particles; **D** is the diameter of the particle.

Table 4. Size survey of ZIF-67 particles (Total synthesis volume 15mL)

Count (n)	Diameter (D μm)
27	1.890
20	2.066
20	2.063
12	2.230
13	1.294
29	1.829
22	2.023
15	1.339
25	1.534
30	1.775
9	1.196

Tips: **n** indicates the number of statistical particles; **D** is the diameter of the particle.

Table 5. Size survey of ZIF-67 particles (Total synthesis volume 60mL)

Count (n)	Diameter (D μm)
17	1.540
12	1.317
8	1.105
12	1.324
17	1.661
12	2.443
17	1.602
19	2.146
14	2.394
7	2.745
10	2.539

Tips: *n* indicates the number of statistical particles; *D* is the diameter of the particle.

sample	pH	etching agent	morphology
ZIF-8 etching	3.92	XO in HCl	Porous
	3.61	XO in HCl	Hollow
ZIF-67 etching	3.61	XO in HCl	Porous
	3.25	XO in HCl	Hollow
	3.09	XO in HCl	Hollow
ZIF-67@ZIF-67 etching	3.09	XO in HCl	Core-shell
ZIF-67@PS etching	3.09	THF	Hollow

Table 6. Summary of ex-situ chemical etching experiments

Table 7. Summary of in-situ chemical etching experiments

sample	pH	etching agent	morphology	Beam dose $e^{-\text{Å}^{-2}\text{s}^{-1}}$
ZIF-8 in-situ etching	3.61	XO in HCl	Hollow	8.4
ZIF-8 in DI water	5.5-6.0	DI water	No shape change	8.7
ZIF-67 in-situ etching	3.61	XO in HCl	Hollow	8.1
	2.39	HF	Broken due to quick etching	8.6
	2.39	XO in HCl	Hollow	8.7

Table 8. Summary of 3D tomography experiments imaging condition

sample	Titling angle range	Step angle	Mag. & Spot size	Beam dose $e^{-\text{Å}^{-2}\text{s}^{-1}}$
ZIF-8 spindle	-42° to 64°	2°	10,000; 6	8.4
ZIF-8 star	-52° to 56°	2°	10,000; 6	8.2
ZIF-67@ZIF-67	-62° to 46°	2°	10,000; 6	8.7

Note: the electron beam dose was calculated by using the following formulation:

$$D = J\Delta t = \left(\frac{4}{\pi}\right)\left(\frac{I_b}{d^2}\right)\Delta t$$

Where $d=d_i/M_i$ can be determined by imaging the specimen plane at a magnification M_i and measuring the image diameter d_i .

Supporting movies

Supporting movie 1: ZIF-8 spindle etching under in-situ liquid phase TEM

Particle size: 1.25 μm

Imaging condition: aqueous acid solution (HCl + XO) with pH = 3.61, movie plays in 4 \times real time.

Note: ZIF-8 synthesis without the present of PVP

Supporting movie 2: ZIF-8 in DI water

Particle size: 2.76 μm

Imaging condition: movie plays in 15 \times real time.

Note: ZIF-8 synthesis without the present of PVP, and this experiment is design to test whether the electron beam leads etching (check size change).

Supporting movie 3: ZIF-67 etching in acid (XO+HCl) solution under in-situ liquid phase TEM

Particle size: 2. 539 μm

Imaging condition: aqueous acid solution (HCl + XO) with pH = 3.61, movie plays in 2 \times real time.

Note: ZIF-8 synthesis without the present of PVP

Supporting movie 4: ZIF-67 etching in acid (HF) solution under in-situ liquid phase TEM

Particle size: 2. 146 μm

Imaging condition: aqueous acid solution (HF) with pH = 3.09, movie plays in 2 \times real time.

Note: ZIF-8 synthesis without the present of PVP

Supporting movie 5: ZIF-67 microbox particle motion under in-situ liquid phase TEM

Particle size: 1.75 μm , movie plays in 2 \times real time

Supporting movie 6: ZIF-67 polyhedral particle motion under in-situ liquid phase TEM

Particle size: 1.75 μm , movie plays in 2 \times real time

Supporting movie 7: ZIF-8 hollow spindle 3D tomography

Supporting movie 8: ZIF-8 hollow star 3D tomography

Supporting movie 9: ZIF 67 hollow core-shell 3D tomography

Supporting references

1. C. Avci, J. Arinez-Soriano, A. Carne-Sanchez, V. Guillerm, C. Carbonell, I. Imaz and D. Maspoch, *Angew Chem Int Ed Engl*, 2015, **54**, 14417-14421.
2. K. Shen, L. Zhang, X. Chen, L. Liu, D. Zhang, Y. Han, J. Chen, J. Long, R. Luque and Y. Li, *Science*, 2018, **359**, 206-210.
3. X. Gong, K. Gnanasekaran, Z. Chen, L. Robison, M. C. Wasson, K. C. Bentz, S. M. Cohen, O. K. Farha and N. C. Gianneschi, *J Am Chem Soc*, 2020, **142**, 17224-17235.
4. X. Gong, K. Gnanasekaran, K. Ma, C. J. Forman, X. Wang, S. Su, O. K. Farha and N. C. Gianneschi, *J Am Chem Soc*, 2022, **144**, 6674-6680.
5. G. Li, H. Zhang and Y. Han, *ACS Cent Sci*, 2022, **8**, 1579-1588.
6. W. Wei, H. Zhang, W. Wang, M. Dong, M. Nie, L. Sun and F. Xu, *ACS Appl Mater Interfaces*, 2019, **11**, 24478-24484.
7. Z. Ou, X. Song, W. Huang, X. Jiang, S. Qu, Q. Wang, P. V. Braun, J. S. Moore, X. Li and Q. Chen, *ACS Appl Mater Interfaces*, 2018, **10**, 40990-40995.
8. M. Hugenschmidt, K. Kutonova, E. P. Valadez Sánchez, S. Moulai, H. Gliemann, S. Bräse, C. Wöll and D. Gerthsen, *Part Part Syst Charact*, 2020, **37**.
9. D. Zhang, Y. Zhu, L. Liu, X. Ying, C.-E. Hsiung, R. Sougrat, K. Li and Y. Han, *Science*, 2018, **359**, 675-679.
10. S. M. Ghodsi, C. M. Megaridis, R. Shahbazian-Yassar and T. Shokuhfar, *Small Methods*, 2019, **3**, 1900026.
11. X. Song, J. W. Smith, J. Kim, N. J. Zaluzec, W. Chen, H. An, J. M. Dennison, D. G. Cahill, M. A. Kulzick and Q. Chen, *ACS Appl Mater Interfaces*, 2019, **11**, 8517-8526.
12. M. R. Hauwiller, J. C. Ondry and A. P. Alivisatos, *J Vis Exp*, 2018, DOI: 10.3791/57665.